Counterdiabatic driving of the quantum Ising model

J. Stat. Mech. (2014) P12019

(http://iopscience.iop.org/1742-5468/2014/12/P12019)

Journal of Statistical Mechanics: Theory and Experiment
An IOP and SISSA journal

Counterdiabatic driving of the quantum Ising model

Bogdan Damski

Institute of Physics, Jagiellonian University, Łojasiewicza 11, 30-348 Kraków, Poland

Received 4 October 2014
Accepted for publication 19 November 2014
Published 22 December 2014

Online at stacks.iop.org/JSTAT/2014/P12019
doi:10.1088/1742-5468/2014/12/P12019

Abstract. A system undergoes adiabatic evolution when its population in the instantaneous eigenbasis of its time-dependent Hamiltonian changes only negligibly. The realization of such dynamics requires slow-enough changes of the parameters of the Hamiltonian, a task that can be hard to achieve near quantum critical points. A powerful alternative is provided by the counterdiabatic modification of the Hamiltonian allowing for an arbitrarily quick implementation of the adiabatic dynamics. Such a counterdiabatic driving protocol has been recently proposed for the quantum Ising model (del Campo *et al* 2012 *Phys. Rev. Lett.* **109** 115703). We derive an exact closed-form expression for all the coefficients of the counterdiabatic Ising Hamiltonian. We discuss two approximations to the exact counterdiabatic Ising Hamiltonian quantifying their efficiency of the dynamical preparation of the desired ground state. In particular, these studies show how quantum criticality enhances finite-size effects in counterdiabatic dynamics.

Keywords: quantum phase transitions (theory), quantum quenches

J. Stat. Mech. (2014) P12019

1742-5468/14/P12019+15$33.00

Contents

J. Stat. Mech. (2014) P12019

1. Introduction

The ability to prepare a quantum system in its ground state is crucial in adiabatic quantum computing [1], quantum simulation of strongly correlated systems with trapped atoms and ions [2,3], studies of macroscopic superpositions of quantum phases in these systems [4–6], etc.

One way to experimentally achieve this goal is to start from an easy to prepare ground state and then drive the system towards the desired ground state that is hard to prepare in a different way. This can be done through a change of the parameter of the Hamiltonian. If such driving is slow enough, the excitation of the system is typically exponentially small in the driving rate [7]. The adiabatic approximation tells us then that the wave-function $|\psi(t)\rangle$ during such evolution will be approximately given by

$$|\psi(t)\rangle = \exp\left(-\mathrm{i}\int_0^t \mathrm{d}t'\varepsilon(t') - \int_0^t \mathrm{d}t'\langle GS(t')|\partial_{t'}GS(t')\rangle\right)|GS(t)\rangle, \tag{1}$$

where $|GS(t)\rangle$ is the (instantaneous) ground state of the system's Hamiltonian $\hat{H}_0[g(t)]$, $\hat{H}_0[g(t)]|GS(t)\rangle = \varepsilon(t)|GS(t)\rangle$ and $g(t)$ is the parameter driving the evolution.

The main limitation of such a procedure comes from the requirement of the slow change of the parameter of the Hamiltonian. The longer the evolution lasts, the more affected by decoherence will be the evolved state. This issue becomes especially troublesome in quantum critical systems, where the vanishing energy gap near the critical point requires prohibitively slow time variations of the driving parameter [8,9].

One way to circumvent this problem is to temporarily modify the system's Hamiltonian such that the adiabatic evolution (1) is strictly imposed regardless of the rate of driving. To achieve that, one adds a counterdiabatic term to the Hamiltonian [10, 11]

$$\hat{H}_1 = \mathrm{i}g'(t)\sum_n \left(|\partial_g n(g)\rangle\langle n(g)| - \langle n(g)|\partial_g n(g)\rangle|n(g)\rangle\langle n(g)|\right), \quad g'(t) = \frac{\mathrm{d}g}{\mathrm{d}t},$$

where $|n(g)\rangle$ are the eigenstates of the system's Hamiltonian $\hat{H}_0[g]$. It is then easy to see that the wave-function (1) satisfies the time-dependent Schrödinger equation

$$\mathrm{i}\frac{\mathrm{d}}{\mathrm{d}t}|\psi(t)\rangle = \hat{H}[g(t)]|\psi(t)\rangle,$$

where the modified Hamiltonian of the system is

$$\hat{H}[g(t)] = \hat{H}_0[g(t)] + \hat{H}_1[g(t)].$$

In fact, not only the ground state but all the other eigenstates of $\hat{H}_0$ undergo a perfect adiabatic evolution with the Hamiltonian $\hat{H}$ no matter how fast the parameter $g(t)$ is changed. A comprehensive discussion of different techniques allowing for a quick preparation of the desired quantum state is presented in a recent review [12]; see also [13, 14]. It is shown there that such techniques—known as shortcuts to adiabaticity—are applicable to both single-particle and many-body systems of atoms, spins, etc.

2. Model

We consider the Ising chain in the transverse field

$$\hat{H}_0 = -\sum_{i=1}^{N}\left(\sigma_i^x\sigma_{i+1}^x + g\sigma_i^z\right), \tag{2}$$

where $\sigma_i^{x,y,z}$ denote the usual Pauli matrices acting on the i-th spin and N is the number of spins in the chain. We assume periodic boundary conditions and choose *even* $N \geqslant 2$ for which the ground state lies in the positive parity subspace [15, 16]. We focus on magnetic fields $g \geqslant 0$. When $g \in [0, 1)$ the system is in the ferromagnetic phase, while for $g \in (1, \infty]$ it is in the paramagnetic phase. The critical point is at the magnetic field $g = 1$. The quantum Ising model is exactly solvable. It is a prototypical model undergoing a quantum phase transition [17, 18]. It serves as a test bed for different theoretical concepts in many-body quantum physics. Besides being of theoretical interest, such a model describes the magnetic properties of cobalt niobate $CoNb_2O_6$ [19]. The number of spins in such a system is thermodynamically large and avoids precise experimental control.

The counterdiabatic term for the quantum Ising model has been found in [20]. It reads

$$\hat{H}_1 = -g'(t)\left(\sum_{m=1}^{N/2-1} h_m(g)H_1^{[m]} + \frac{1}{2}h_{N/2}(g)H_1^{[N/2]}\right), \tag{3}$$

where each term

$$\hat{H}_1^{[m]} = \sum_{n=1}^{N}\left[\sigma_n^x\left(\prod_{j=n+1}^{n+m-1}\sigma_j^z\right)\sigma_{n+m}^y + \sigma_n^y\left(\prod_{j=n+1}^{n+m-1}\sigma_j^z\right)\sigma_{n+m}^x\right],$$

J. Stat. Mech. (2014) P12019

describes interactions of $m+1$ adjoint spins. Thus, to implement the counterdiabatic protocol one needs to be able to: (i) prepare an Ising chain with a predefined number of spins; (ii) implement the multi-spin interaction terms. The former should be available in the near future in cold ion [21, 22], cold atom [23] and nuclear magnetic resonance [24] simulators of spin systems. The latter is even more demanding, but may be possible with the techniques proposed in [25].

The coefficients providing the strength of the $(m+1)$-body interaction terms are given by[1]

$$h_m(g) = \frac{1}{2N}\sum_k \frac{\sin(k)\sin(mk)}{g^2 - 2g\cos(k) + 1}, \tag{4}$$

where both here and everywhere below

$$k = \frac{\pi}{N}, \frac{3\pi}{N}, \cdots, \pi - \frac{\pi}{N}.$$

It has been proposed in [20] that in the thermodynamic limit one can approximate the exact coefficients with

$$\tilde{h}_m(g) = \frac{1}{8}\begin{cases} g^{m-1} & \text{for } 0 \leqslant g < 1 \\ g^{-m-1} & \text{for } g \geqslant 1 \end{cases}. \tag{5}$$

This article is organized as follows. Section 3 is devoted to the derivation of the exact closed-form expression for all the $h_m(g)$ coefficients and to the discussion of how they reflect the symmetries of the quantum Ising model. Sections 4 and 5 discuss two approximations to the exact counterdiabatic Hamiltonian. The former studies the dynamics induced by the interaction-truncated counterdiabatic Hamiltonian, while the latter focuses on the dynamics resulting from the thermodynamic approximation (5). In both sections, we quantify the efficiency of the dynamical preparation of the desired ground states. Our findings are briefly summarized in section 6.

3. Exact counterdiabatic coefficients

We will prove in this section the exact closed-form expression for $h_m(g)$ coefficients, the remarkably compact formula:

$$h_m(g) = \frac{g^{2m} + g^N}{8g^{m+1}(1+g^N)} - \frac{\delta_{m0}}{8g}, \tag{6}$$

for $m = 0, 1, \cdots, N-1$, where the trivial $m = 0$ case is added to simplify the subsequent calculations.

To prove it, we define one additional sum

$$f_m(g) = \frac{1}{2N}\sum_k \frac{\cos(mk)}{g^2 - 2g\cos(k) + 1}, \tag{7}$$

and conjecture that

$$f_m(g) = \frac{1}{4g^m}\frac{g^N - g^{2m}}{(g^N+1)(g^2-1)}, \tag{8}$$

[1] The 1/2 prefactor in equation (4) differs from the 1/4 prefactor in the expression for $h_m(g)$ in [20] because we sum over positive momenta k only, while the summation in [20] goes over positive and negative momenta, i.e. $\pm k$ in our notation.

for $m = 0, 1, \cdots, N-1$. The reasoning leading to these two conjectures, equations (6) and (8), is explained in appendix A. We will now simultaneously prove equations (6) and (8) by mathematical induction.

First, we stress that equations (6) and (8) are correct for even $N \geqslant 2$ only. Moreover, it is worth noting that all we need for the counterdiabatic Hamiltonian is the expression for the $h_m(g)$ coefficients for $m \leqslant N/2$, so we will prove a more general result. Finally, we mention that although we assume $g > 0$ in the proof, equations (6) and (8) work for $g < 0$ as well. Indeed, from equations (4) and (7) one gets that $h_m(-g) = (-)^{m+1} h_m(g)$ and $f_m(-g) = (-)^m f_m(g)$. The same $g \leftrightarrow -g$ mapping is exhibited by equations (6) and (8).

The induction starts from $m = 0$, where we find that indeed equations (6) and (8) hold: The former holds trivially, while the latter immediately follows from the following identity provided in section 1.382 of [26]

$$\sum_k \left[\frac{\sin^2(k/2)}{\sinh(x)} + \frac{\tanh(x/2)}{2} \right]^{-1} = N \tanh\left(\frac{Nx}{2}\right), \tag{9}$$

after substituting $x = \ln(g)$.

Second, we use equations (4) and (7) to show that

$$\begin{aligned} h_{m+1}(g) &= \frac{g^2+1}{2g} h_m(g) - \left[\frac{g^2-1}{2g}\right]^2 f_m(g) + \frac{g^2+1}{16g^2}\delta_{m0}, \\ f_{m+1}(g) &= \frac{g^2+1}{2g} f_m(g) - h_m(g) - \frac{\delta_{m0}}{8g}. \end{aligned} \tag{10}$$

From these relations it is clear why we have to consider the additional series, $f_m(g)$, to inductively prove the conjectured expression for $h_m(g)$. Equations (10) can be written in such a compact form with the help of the following identities valid for integer $m \in [0, N-2]$

$$\frac{1}{2N} \sum_k \frac{\cos(mk)\cos(k)}{g^2 - 2g\cos(k) + 1} = \frac{g^2+1}{2g} f_m(g) - \frac{\delta_{m0}}{8g}, \tag{11}$$

$$\frac{1}{2N} \sum_k \frac{\cos(mk)\sin^2(k)}{g^2 - 2g\cos(k) + 1} = -\left[\frac{g^2-1}{2g}\right]^2 f_m(g) + \frac{g^2+1}{16g^2}\delta_{m0} + \frac{\delta_{m1}}{16g}, \tag{12}$$

$$\frac{1}{2N} \sum_k \frac{\sin(mk)\sin(k)\cos(k)}{g^2 - 2g\cos(k) + 1} = \frac{g^2+1}{2g} h_m(g) - \frac{\delta_{m1}}{16g}. \tag{13}$$

Equations (11)–(13) are derived in appendix B.

Third, substituting equations (6) and (8) into equations (10) one finds that

$$h_{m+1}(g) = \frac{g^{2m+2} + g^N}{8g^{m+2}(1+g^N)}, \quad f_{m+1}(g) = \frac{1}{4g^{m+1}} \frac{g^N - g^{2m+2}}{(g^N+1)(g^2-1)},$$

which agrees with the conjectured expressions (6) and (8) taken at $m+1$. Such inductive reasoning can be carried out for $m = 0, 1, \cdots, N-2$, for which equations (11)–(13) hold. This concludes the inductive proof that equations (6) and (8) are valid for $m = 0, 1, \cdots, N-1$. Note that the largest m for which one can inductively prove equation (6) is indeed $N-1$, because equation (6) clearly gives a wrong result for $m = N$. We will now point out some general features of expression (6).

J. Stat. Mech. (2014) P12019

The $h_m(g)$ coefficients follow a simple law under the Kramers–Wannier duality transformation (this symmetry of the quantum Ising model is discussed in [27])

$$g \leftrightarrow \frac{1}{g}.$$

Indeed, using equation (6) one easily finds that

$$g h_m(g) = \frac{1}{g} h_m\left(\frac{1}{g}\right). \tag{14}$$

This equation provides the ferromagnetic/paramagnetic duality of the $h_m(g)$ coefficients, i.e. a one-to-one mapping between their values in the ferromagnetic and paramagnetic phases. Thus, equation (14) explicitly shows how the counterdiabatic Hamiltonian reflects the symmetry of the system for which it is written. Moreover, we mention that duality symmetry (14) implies that the maximum of the $h_m(g)$ coefficients is not at the quantum critical point in any finite Ising chain (2). This follows from the observation that one can rewrite equation (14) to the form

$$h_m(g) = \frac{\varphi_m(g)}{g}, \quad \varphi_m(g) = \varphi_m\left(\frac{1}{g}\right). \tag{15}$$

Since $\mathrm{d}\varphi_m(g)/\mathrm{d}g = 0$ at $g = 1$, $\mathrm{d}h_m(g)/\mathrm{d}g$ cannot be equal to zero at the critical point. The $1/g$ factor in equation (15) shifts the maximum into the ferromagnetic phase, which can be directly verified from equation (6) as well.

A similar symmetry property has been found in the studies of the related quantity, fidelity susceptibility providing the overlap of two 'nearby' ground states [28]. Just like $h_m(g)$, fidelity susceptibility is peaked near the critical point [29,30]. Besides the location of the critical point, it encodes the universal critical exponent ν providing the scaling of the correlation length $\xi(g)$ with the distance from the critical point [16]. We can see here the influence of quantum criticality by noting that $h_m(g)$ depends on m and N through the combinations

$$g^m = \exp\left(\pm\frac{m}{\xi(g)}\right), \quad g^N = \exp\left(\pm\frac{N}{\xi(g)}\right), \tag{16}$$

where

$$\xi(g) = 1/|\ln(g)| \approx |g-1|^{-1}$$

is the correlation length of the quantum Ising model [31]; upper/lower sign corresponds to the paramagnetic/ferromagnetic phase. The first of these relations has been noted in [20] as it is properly captured by the thermodynamic approximation (5). Assuming that the divergence of the correlation length near the critical point g_c is given by the standard expression

$$\xi(g) \sim |g - g_c|^{-\nu}, \tag{17}$$

one may speculate that the magnitude of the $(m+1)$-body counterdiabatic interactions in other critical systems will depend on the interaction range and the system size through the combinations $m|g-g_c|^{\nu}$ and $N|g-g_c|^{\nu}$. It would be interesting to verify this simple conjecture.

J. Stat. Mech. (2014) P12019

4. Truncated counterdiabatic dynamics

The main complications in the experimental implementation of counterdiabatic dynamics should come from the need to engineer the multi-spin interactions. Suppose now that we can implement only the counterdiabatic terms coupling up to $M+1$ spins, i.e. we substitute

$$\bar{h}_m(g) = \begin{cases} \dfrac{g^{2m}+g^N}{8g^{m+1}(1+g^N)} & \text{for } \ 1 \leqslant m \leqslant M \\ 0 & \text{for } \ m > M \end{cases} \tag{18}$$

for $h_m(g)$ in the Hamiltonian (3). If $M = N/2$ the full counterdiabatic protocol is implemented and an exact preparation of the desired ground state takes place. In the opposite limit, i.e. when $M = 0$, the whole counterdiabatic Hamiltonian disappears and we are left with the system susceptible to the non-adiabatic dynamics across the critical point [32, 33]. The purpose of this section is to quantify the probability of finding the system in the ground state by the end of time evolution, if the dynamics is driven by the truncated counterdiabatic Hamiltonian. The study of the density of defects created due to the truncation of the counterdiabatic Hamiltonian was performed in [20]. Thus, our work provides a complementary insight into the influence of the truncation on the dynamics of the Ising chain. It is worth mentioning that a different simplification of the counterdiabatic Ising Hamiltonian has been recently discussed in [34].

The time-dependent modulation of the magnetic field is chosen such that at the beginning and the end of the time evolution—$t = 0$ and $t = T$, respectively—$\hat{H} = \hat{H}_0[g(t)]$. Moreover, we assume that the magnetic field changes from g_0 to g_f. These requirements impose the following boundary conditions

$$g(0) = g_0, \quad g'(0) = 0, \quad g(T) = g_f, \quad g'(T) = 0.$$

They are satisfied, for example, by a simple polynomial ansatz of the form

$$g(t) = g_0 + 3\,(g_f - g_0)\left(\frac{t}{T}\right)^2 - 2\,(g_f - g_0)\left(\frac{t}{T}\right)^3, \tag{19}$$

which we will use below. Such an ansatz has been used in previous studies as well [34]. We start the evolution from $g_0 = 5$, i.e. far away from the critical point in the paramagnetic phase and evolve the system deeply into the ferromagnetic phase all the way to $g_f = 0$. This is the typical setup for the studies of the dynamics of the quantum Ising chain (see e.g. [20, 32, 33]).

Although the experimental implementation of the counterdiabatic Hamiltonian (3) is challenging due to the presence of the multi-spin interactions, the theoretical description of the dynamics of the system driven by the non-local counterdiabatic Hamiltonian is straightforward. This is seen by performing the Jordan–Wigner transformation:

$$\sigma_n^z = 1 - 2\hat{c}_n^\dagger \hat{c}_n, \quad \sigma_n^x + \mathrm{i}\sigma_n^y = 2\hat{c}_n \prod_{l<n}\left(1 - 2\hat{c}_l^\dagger \hat{c}_l\right),$$

where $\hat{c}_n$ are fermionic operators and then going to the momentum space through the substitution

$$\hat{c}_n = \frac{\exp(-\mathrm{i}\pi/4)}{\sqrt{N}} \sum_{K=\pm k} \hat{c}_K \exp(\mathrm{i}Kn).$$

J. Stat. Mech. (2014) P12019

After these transformations one obtains

$$\hat{H} = 2\sum_k \hat{\psi}_k^\dagger \left[\sin(k)\sigma^x - g'(t)q_k(g)\sigma^y - (\cos(k) - g)\,\sigma^z\right]\hat{\psi}_k, \quad \hat{\psi}_k = \begin{pmatrix} \hat{c}_k \\ \hat{c}_{-k}^\dagger \end{pmatrix},$$

where

$$q_k(g) = 2\sum_{m=1}^{N/2-1} h_m(g)\sin(km) + h_{N/2}(g)\sin(kN/2). \tag{20}$$

The evolution starts from a ground state of the Ising Hamiltonian, i.e. from a product state

$$|GS(g)\rangle = \prod_k \left(\cos\left(\frac{\theta_k}{2}\right) - \sin\left(\frac{\theta_k}{2}\right)\hat{c}_k^\dagger \hat{c}_{-k}^\dagger\right)|\text{vac}\rangle,$$

$$\sin\theta_k = \frac{\sin(k)}{\sqrt{g^2 - 2g\cos(k) + 1}}, \quad \cos\theta_k = \frac{g - \cos(k)}{\sqrt{g^2 - 2g\cos(k) + 1}}$$

taken at $g = g_0$. The $|\text{vac}\rangle$ state is annihilated by all $\hat{c}_k$ operators.

Solving the Schrödinger equation $\mathrm{i}\frac{\mathrm{d}}{\mathrm{d}t}|\psi(t)\rangle = \hat{H}[g(t)]|\psi(t)\rangle$ with the initial wavefunction $|\psi(t=0)\rangle = |GS(g_0)\rangle$, one finds that

$$|\psi(t)\rangle = \prod_k \left(u_k(t) - v_k(t)\hat{c}_k^\dagger \hat{c}_{-k}^\dagger\right)|\text{vac}\rangle,$$

$$\mathrm{i}\frac{\mathrm{d}}{\mathrm{d}t}\begin{pmatrix} v_k \\ u_k \end{pmatrix} = 2\begin{pmatrix} g - \cos(k) & -\sin(k) - \mathrm{i}g'(t)q_k \\ -\sin(k) + \mathrm{i}g'(t)q_k & \cos(k) - g \end{pmatrix}\begin{pmatrix} v_k \\ u_k \end{pmatrix}.$$

If we substitute the exact $h_m(g)$ into equation (20), we get

$$q_k(g) = \frac{1}{4}\frac{\sin(k)}{g^2 - 2g\cos(k) + 1}, \tag{21}$$

which guarantees the perfect preparation of the ground state by the end of time evolution [20]. Namely,

$$p_{GS} = |\langle\psi(T)|GS(g_f)\rangle|^2$$

equals unity in such a case. What happens when we use coefficients (18) instead of (6) is plotted in figure 1. Several comments are now in order.

First, when $M = N/2$, no truncation is involved, the perfect preparation of the ground state happens. Therefore, p_{GS} should be equal to one. Our numerical simulations provide $|p_{GS} - 1| = \mathrm{O}\,(10^{-12})$ for all the $M = N/2$ cases illustrated in figure 1. This shows that the numerical errors are negligible in our computations.

Second, we consider the $M = 0$ case, when counterdiabatic dynamics is absent. We see that the probability of finding the system in the ground state quickly goes to zero as the system size increases. The need to counteract this tendency motivates the introduction of the counterdiabatic driving protocol that we have discussed. It should be said that this disappearance of p_{GS} comes from the fact that the gap in the excitation spectrum scales as $1/N$ near the critical point. As a result, bigger systems get more excited due to the dynamical crossing of the critical point. The excitations that are created in the course of such dynamics are known as kinks (see e.g. [32, 33]).

Third, for large enough systems—N larger than a few tens for the evolutions from figure 1—we find that p_{GS} depends mostly on the m/N ratio (see the lower panel). Using

J. Stat. Mech. (2014) P12019

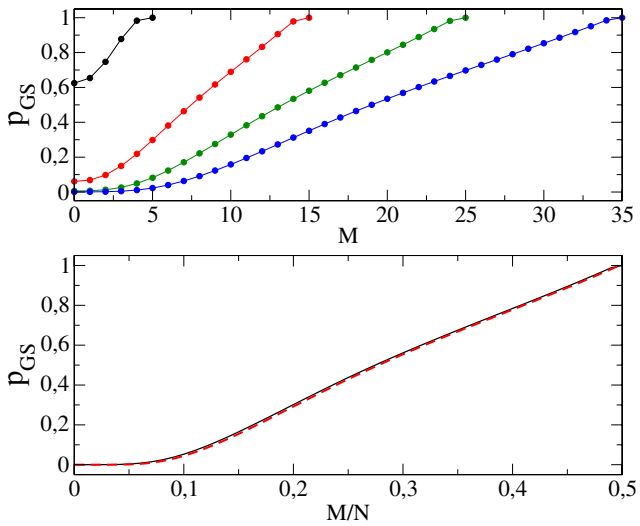

Figure 1. The probability of finding the system in the ground state by the end of time evolution as a function of the range of counterdiabatic interactions (18). Upper panel: lines from left to right correspond to N equal to 10 (black), 30 (red), 50 (green), 70 (blue). Lower panel: solid black line corresponds to $N = 100$ while the red dashed line to $N = 200$. The evolutions are driven by the time-dependent magnetic field (19), where $g_0 = 5$, $g_f = 0$ and $T = 10$.

figure 1, we can correlate the range of the counterdiabatic interactions with the probability of ground state preparation. On the one hand, we notice that even the substantially truncated counterdiabatic Hamiltonian greatly increases p_{GS} with respect to what one ends up with when no counterdiabatic driving is present. On the other hand, to prepare the desired ground state with probability larger than 95%, virtually all the terms in the counterdiabatic Hamiltonian have to be present. This observation quantifies how demanding the counterdiabatic dynamics is if high-probability of ground state preparation is sought.

5. Thermodynamic approximation

We will discuss here the thermodynamic approximation (5) to the counterdiabatic Hamiltonian to illustrate the interplay between finite-size effects and quantum criticality in counterdiabatic dynamics.

The numerics is performed in the same way as in the previous section, except we use the coefficients $\tilde{h}_m(g)$ instead of $\bar{h}_m(g)$. The system-size dependence of the probability of ground state preparation p_{GS} is illustrated in figure 2. This figure shows that the lack of finite-size effects in the counterdiabatic coefficients limits the maximum efficiency of the preparation of the ground state.

On the other hand, the efficiency of the driving with the thermodynamic Hamiltonian is quite substantial and equals about 96% in the large system limit (figure 2). This can be compared to the truncation approximation studied in section 4. To achieve the same probability of the ground state preparation with the latter approach, one needs to perfectly emulate all but one or two longest-range interaction terms (figure 1).

J. Stat. Mech. (2014) P12019

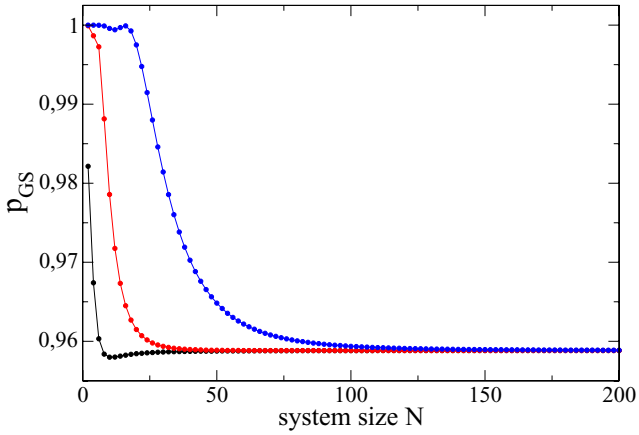

Figure 2. The probability of finding the system in the ground state by the end of time evolution as a function of the system size. Thermodynamically-approximated coefficients (5) are used in the counterdiabatic Hamiltonian (3). The evolutions are driven by the time-dependent magnetic field (19), where $g_0 = 5$ and $g_f = 0$. The black, red and blue lines—bottom to top—correspond to the evolution times T equal to 1, 10 and 100, respectively.

The fact that p_{GS} obtained through the thermodynamic approximation does not approach unity as the system size increases is a bit surprising. In fact, it has an interesting explanation that we will provide below.

The thermodynamic approximation (5) follows from the replacement of the sum by the integral in equation (4)

$$\sum_k \to \frac{N}{2\pi}\int_0^\pi \mathrm{d}k.$$

We expect that such an approximation will work well when $m/N \ll 1$ and that it will fail for m of the order of $N/2$. This expectation is based on the observation that when $k \to k+2\pi/N$, the summand in equation (4) changes slowly in the former case and quickly in the latter one. Since there are simple analytical expressions for the thermodynamic (5) and exact (6) $h_m(g)$ coefficients, the reader can easily verify these expectations. We illustrate this in figure 3.

Next, we substitute the $\tilde{h}_m(g)$ coefficients into equation (20) to see how the inaccuracies of the thermodynamic approximation affect time evolution. We get

$$q_k(g) = \frac{1}{4}\frac{\sin(k)}{g^2 - 2g\cos(k) + 1} \pm \frac{g^{\pm N/2}}{8g}\frac{g^2-1}{g^2 - 2g\cos(k) + 1}\sin(kN/2), \qquad (22)$$

where the upper/lower sign should be used in the ferromagnetic/paramagnetic phase. The first term in this expression reproduces the exact form of the $q_k(g)$ factor (21) needed for a perfect adiabatic preparation of any eigenstate of the Ising Hamiltonian (2). The second one is the correction resulting from the above-described deficiencies of the thermodynamic approximation. Rewriting $g^{\pm N/2}$ as $\exp(-N/2\xi(g))$, we see that this correction plays a role only in the quantum critical regime, where the correlation length $\xi(g)$ is comparable to or greater than the system size N [note that this is possible as $\xi(g)$ stands for the correlation length of the infinite system (17)].

J. Stat. Mech. (2014) P12019

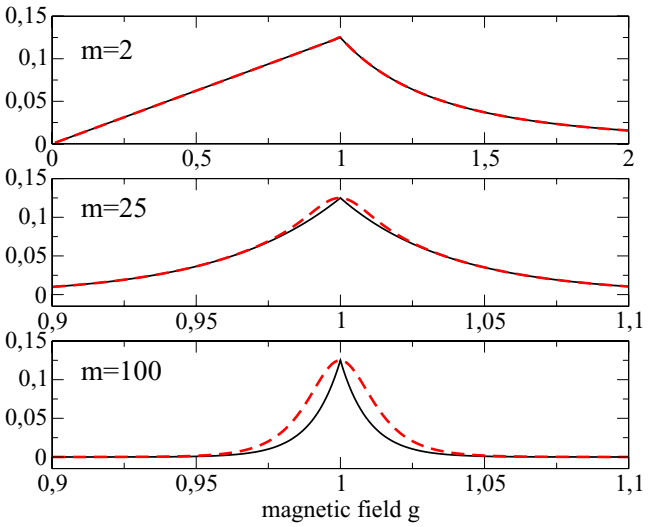

Figure 3. Exact $h_m(g)$ versus approximate $\tilde{h}_m(g)$ coefficients. Exact results (red dashed line) come from equation (6), while the thermodynamic approximation (black solid line) is provided by equation (5). The number of spins $N = 200$.

This gives us the following picture of the dynamics driven by the thermodynamically-approximated counterdiabatic Hamiltonian. Suppose that the evolution starts far away from the critical point in the paramagnetic phase. The population of the instanteneous eigenstates of the time-dependent Ising Hamiltonian (2) does not change until we reach the neighborhood of the critical point, where $|g-1| = \mathrm{O}(1/N)$. For such magnetic fields the second term in equation (22) excites the system. Soon after leaving the neighborhood of the critical point, the adiabatic dynamics resumes and the excited system is driven without a change of its population in the instantaneous eigenbasis. This is illustrated in figure 4.

6. Discussion

We have found the exact closed-form expression for all the coefficients of the counterdiabatic Ising Hamiltonian (6). Our results are very compact and provide the ultimate simplification of this Hamiltonian. We have discussed how the Kramers–Wannier duality and quantum critical properties of the Ising chain are imprinted onto the counterdiabatic Hamiltonian (14), (16). It should be stressed that our equations (6) and (8) provide neat summation formulas that can be used in other contexts as well.

The main complications in the experimental implementation of the counterdiabatic Hamiltonian come from its reliance on the many-body interactions that are hard-to-induce in real physical systems. We have truncated the exact counterdiabatic Hamiltonian removing its longest-range interaction terms. Using such a Hamiltonian, we have quantified the efficiency of the preparation of the desired ground state. We have shown that the truncated Hamiltonian can significantly improve the probability of finding the system in the ground state by the end of time evolution. However, if the goal is to prepare the ground state with a substantial probability, say greater than 95%, then this approximation

J. Stat. Mech. (2014) P12019

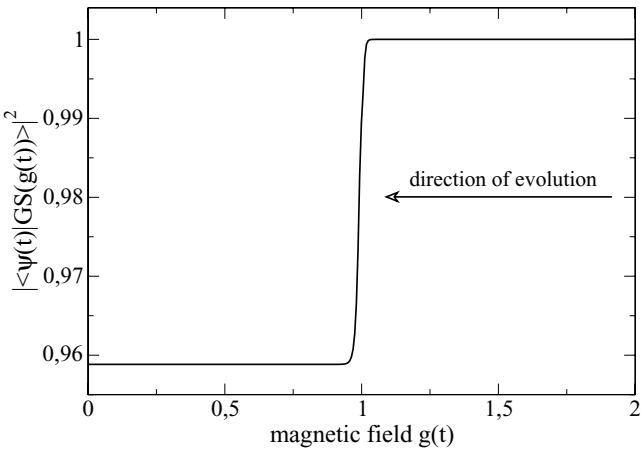

Figure 4. The probability of finding the system in the instantaneous ground state during time evolution from the paramagnetic to the ferromagnetic phase. Thermodynamically-approximated coefficients (5) are used in the counterdiabatic Hamiltonian (3). The evolution is driven by the time-dependent magnetic field (19), where $g_0 = 5$, $g_f = 0$ and $T = 10$. The system size $N = 200$. Compare this figure to figures 2 and 3.

becomes inefficient as virtually all the multi-spin interaction terms have to be kept to achieve such a goal.

We have considered a simple thermodynamic approximation to the counterdiabatic Hamiltonian coefficients and explained its limited efficiency in the dynamical preparation of the desired ground state. It should be noted that there is no incentive to actually use that approximation given the compactness of our exact result (6). We think, however, that the study of this approximation provides some insights into the role of the finite-size effects in counterdiabatic dynamics. It shows that the thermodynamic approximation leads to the undesired excitation of the system in the quantum critical regime, where finite-size effects cannot be overlooked if one aims at high-probability preparation of the target ground state.

Acknowledgments

This work has been supported by the Polish National Science Centre (NCN) grant DEC-2013/09/B/ST3/00239. I would like to thank Adolfo del Campo for several useful suggestions and stimulating discussions.

Appendix A. Conjecture

We describe below how one can conjecture fairly complicated equations (6) and (8). The main difficulty here is that equations (4) and (7) depend on both the system size N and the range of counterdiabatic interactions m. In the following, we factor out the N-dependence exactly, leaving the m-dependence for an easy educated guess. We focus on showing the key steps in this calculation leaving the details to the reader.

J. Stat. Mech. (2014) P12019

First, we notice that the denominator in equation (4) can be rewritten as

$$g^2 - 2g\cos(k) + 1 = 4g\left[\sin^2(k/2) + \sinh^2(x/2)\right], \tag{A1}$$

where $x = \ln(g)$. The calculations can be more efficiently performed in the x-parameterization.

Second, we derive the recurrence relation for

$$w_n = \sum_k \frac{\sin^n(k/2)}{\sin^2(k/2) + \sinh^2(x/2)},$$

which reads

$$w_{2n+2} = \frac{N}{2^{2n+1}}\binom{2n}{n} - w_{2n}\sinh^2(x/2), \quad n = 0, 1, \cdots, N-1. \tag{A2}$$

To solve this relation, we find from identity (9) that

$$w_0(x) = N\frac{\tanh(Nx/2)}{\sinh(x)}. \tag{A3}$$

Note that this equation is valid for even $N \geqslant 2$, which we assume throughout this article. Combining equations (A2) and (A3) we get

$$\sum_k \frac{\sin^{2n}(k/2)}{\sin^2(k/2) + \sinh^2(x/2)} = N(-)^n \sinh^{2n}(x/2)\frac{\tanh(Nx/2)}{\sinh(x)} + N\sum_{s=0}^{n-1}\binom{2s}{s}\frac{(-)^{n-s-1}}{2^{2s+1}}\sinh^{2n-2s-2}(x/2), \tag{A4}$$

which is valid for $n = 0, 1, \cdots, N$ (the sum on the right-hand side yields zero for $n = 0$).

Third, we expand the numerator in equation (4). We obtain

$$\sin(k)\sin(mk) = \sum_{s=0}^{m}\mathcal{A}_s^m \sin^{2s+2}(k/2), \quad \mathcal{A}_s^m = (-)^s 2^{2s+1}\frac{(m+s-1)!}{(m-s)!(2s+1)!}\left(2m^2 + s\right) \tag{A5}$$

for $m > 0$ ($\mathcal{A}_0^0 = 0$). Taking $x = \ln(g)$ and combining equations (A4) and (A5), we find that

$$h_m(g) = \frac{1}{8g}\sum_{j=0}^{m}(-)^j\mathcal{A}_j^m\left[\frac{(g-1)^2}{4g}\right]^j\left(\frac{g^N+g}{(g+1)(g^N+1)} + \sum_{s=1}^{j}\binom{2s}{s}\frac{(-)^s}{2^{2s+1}}\left[\frac{4g}{(g-1)^2}\right]^s\right) \tag{A6}$$

for $m = 1, 2, \cdots, N-1$. This equation is fairly complicated and we do not know how to simplify it. It has, however, the N-dependence in a closed form, which greatly facilitates the following considerations. Substituting $m = 1, 2, \cdots$ into equation (A6) one easily guesses that the general expression for $h_m(g)$ is provided by equation (6). It should be stressed that it would be very difficult to conjecture equation (6) right from equation (4).

Fourth, we expand the numerator in equation (7) getting

$$\cos(mk) = \sum_{s=0}^{m}\mathcal{B}_s^m \sin^{2s}(k/2), \quad \mathcal{B}_s^m = \frac{(-)^s 2^{2s} m(m+s-1)!}{(m-s)!(2s)!} \tag{A7}$$

J. Stat. Mech. (2014) P12019

for $m > 0$ ($\mathcal{B}_0^0 = 1$). Taking again $x = \ln(g)$ and this time combining equations (A4) and (A7), we get

$$f_m(g) = \frac{1}{8g}\sum_{j=0}^{m}(-)^j\mathcal{B}_j^m\left[\frac{(g-1)^2}{4g}\right]^j\left(\frac{2g}{g^2-1}\frac{g^N-1}{g^N+1} - \sum_{s=0}^{j-1}\binom{2s}{s}\frac{(-)^s}{2^{2s+1}}\left[\frac{4g}{(g-1)^2}\right]^{s+1}\right)$$

for $m = 1, 2, \cdots, N-1$. As before, substituting $m = 1, 2, \cdots$ we quickly find that equation (8) is a good candidate for an exact expression for series (7).

Appendix B. Auxiliary sums

Derivation of equation (11). We employ the x-parameterization from equation (A1). After elementary manipulations we find that

$$\frac{\mathrm{d}}{\mathrm{d}z}\left[\sinh^2(z/2)\sum_k\frac{\cos(mk)}{\sin^2(k/2)+\sinh^2(z/2)}\right] = -\frac{1}{2}\frac{\mathrm{d}}{\mathrm{d}z}\sum_k\frac{\cos(mk)\,[1-\cos(k)]}{\sin^2(k/2)+\sinh^2(z/2)}.$$

Integrating it over z from 0 to x we get

$$\sum_k\frac{\cos(mk)\cos(k)}{\sin^2(k/2)+\sinh^2(x/2)} = \cosh(x)\sum_k\frac{\cos(mk)}{\sin^2(k/2)+\sinh^2(x/2)} - N\Delta_m,$$

$$\Delta_m = \begin{cases} 0 & \text{for } \dfrac{m}{N}\notin\mathbb{Z} \\ (-1)^{m/N} & \text{for } \dfrac{m}{N}\in\mathbb{Z}, \end{cases}$$

where $N\Delta_m$ comes from the evaluation of $2\sum_k\cos(mk)$ and $\mathbb{Z} = 0, \pm1, \pm2, \cdots$. Substituting $x = \ln(g)$ and restricting the range of m to $[0, N-2]$ we obtain equation (11).

Derivation of equation (12). Just as above, one finds that

$$\frac{\mathrm{d}}{\mathrm{d}z}\left[\sinh^2(z/2)\sum_k\frac{\cos(mk)\cos(k)}{\sin^2(k/2)+\sinh^2(z/2)}\right] = -\frac{1}{2}\frac{\mathrm{d}}{\mathrm{d}z}\sum_k\frac{\cos(mk)\cos(k)\,[1-\cos(k)]}{\sin^2(k/2)+\sinh^2(z/2)}.$$

Repeating the same steps as above, we get

$$\sum_k\frac{\cos(mk)\sin^2(k)}{\sin^2(k/2)+\sinh^2(x/2)} = -\sinh^2(x)\sum_k\frac{\cos(mk)}{\sin^2(k/2)+\sinh^2(x/2)} + N\cosh(x)\Delta_m + \frac{N}{2}\left(\Delta_{m-1}+\Delta_{m+1}\right),$$

which is equivalent to equation (12) for $x = \ln(g)$ and integer $m \in [0, N-2]$.

Derivation of equation (13). This time we start from

$$\frac{\mathrm{d}}{\mathrm{d}z}\left[\sinh^2(z/2)\sum_k\frac{\sin(k)\sin(mk)}{\sin^2(k/2)+\sinh^2(z/2)}\right] = -\frac{1}{2}\frac{\mathrm{d}}{\mathrm{d}z}\sum_k\frac{\sin(k)\sin(mk)\,[1-\cos(k)]}{\sin^2(k/2)+\sinh^2(z/2)}$$

and end up with

$$\sum_k\frac{\sin(k)\sin(mk)\cos(k)}{\sin^2(k/2)+\sinh^2(x/2)} = \cosh(x)\sum_k\frac{\sin(k)\sin(mk)}{\sin^2(k/2)+\sinh^2(x/2)} - \frac{N}{2}\left(\Delta_{m-1}-\Delta_{m+1}\right),$$

which can be transformed into equation (13) by taking $x = \ln(g)$ and integer $m \in [0, N-2]$.

J. Stat. Mech. (2014) P12019

References

[1] Farhi E *et al* 2001 *Science* **292** 472
[2] Lewenstein M, Sanpera A and Ahufinger V 2012 *Ultracold Atoms in Optical Lattices: Simulating Quantum Many-Body Systems* (New York: Oxford University Press)
[3] Bloch I, Dalibard J and Nascimbène S 2012 *Nat. Phys.* **8** 267
Blatt R and Roos C F 2012 *Nat. Phys.* **8** 277
[4] Rams M M, Zwolak M and Damski B 2012 *Sci. Rep.* **2** 655
[5] Baltrusch J D, Cormick C, De Chiara G, Calarco T and Morigi G 2011 *Phys. Rev.* A **84** 063821
[6] Maschler C and Ritsch H 2005 *Phys. Rev. Lett.* **95** 260401
[7] Dykhne A M 1962 *Sov. Phys.—JETP* **14** 941
Hwang J-T and Pechukas P 1977 *J. Chem. Phys.* **67** 4640
[8] Dziarmaga J 2010 *Adv. Phys.* **59** 1063
[9] Polkovnikov A, Sengupta K, Silva A and Vengalattore M 2011 *Rev. Mod. Phys.* **83** 863
[10] Demirplak M and Rice S A 2003 *J. Phys. Chem.* A **107** 9937
[11] Berry M V 2009 *J. Phys. A: Math. Theor.* **42** 365303
[12] Torrontegui E *et al* 2013 *Adv. At. Mol. Opt. Phys.* **62** 117
[13] Deffner S, Jarzynski C and del Campo A 2014 *Phys. Rev.* X **4** 021013
[14] del Campo A and Sengupta K 2014 arXiv:1409.8301 (*Eur. Phys. J.* at press)
[15] Damski B and Rams M M 2014 *J. Phys. A: Math. Theor.* **47** 025303
[16] Albuquerque A F, Alet F, Sire C and Capponi S 2010 *Phys. Rev.* B **81** 064418
[17] Sachdev S and Keimer B 2011 *Phys. Today* **64** 29
[18] Sachdev S 2011 *Quantum Phase Transitions* (Cambridge: Cambridge University Press)
[19] Coldea R *et al* 2010 *Science* **327** 177
[20] del Campo A, Rams M M and Zurek W H 2012 *Phys. Rev. Lett.* **109** 115703
[21] Kim K *et al* 2011 *New J. Phys.* **13** 105003
Korenblit S *et al* 2012 *New J. Phys.* **14** 095024
Islam R *et al* 2013 *Science* **340** 583
Richerme P, Senko C, Smith J, Lee A, Korenblit S and Monroe C 2013 *Phys. Rev.* A **88** 012334
[22] Lanyon B P 2011 *Science* **334** 57
[23] Simon J, Bakr W S, Ma R, Tai M E, Preiss P M and Greiner M 2011 *Nature* **472** 307
[24] Li Z *et al* 2014 *Phys. Rev. Lett.* **112** 220501
[25] Casanova J, Mezzacapo A, Lamata L and Solano E 2012 *Phys. Rev. Lett.* **108** 190502
[26] Gradshteyn I S and Ryzhik I M 2007 *Table of Integrals, Series and Products* 7th edn (New York: Academic Press)
[27] Fradkin E and Susskind L 1978 *Phys. Rev.* D **17** 2637
[28] Damski B 2013 *Phys. Rev.* E **87** 052131
[29] Gu S-J 2010 *Int. J. Mod. Phys.* B **24** 4371
[30] Gu S-J and Yu W C 2014 *Europhys. Lett.* **108** 20002
[31] Barouch E and McCoy B M 1971 *Phys. Rev.* A **3** 786
[32] Zurek W H, Dorner U and Zoller P 2005 *Phys. Rev. Lett.* **95** 105701
[33] Dziarmaga J 2005 *Phys. Rev. Lett.* **95** 245701
[34] Saberi H, Opatrný T, Mølmer K and del Campo A 2014 *Phys. Rev.* A **90** 060301(R)

J. Stat. Mech. (2014) P12019